JOURNAL OF OPTOELECTRONICS AND ADVANCED MATERIALS, Vol. 10, No. 12, December 2008, p. 3251 - 3256

Deposition of oriented nanocrystalline TiO_2 thin films

DEEPAK R. PATIL*, LALIT S. PATIL, JASPAL P. BANGE, D. K. GAUTAM
Department of Electronics, North Maharashtra University, PB # 80, Jalgaon – 425 001 (M.S.) India

Titanium dioxide (TiO_2) thin films were deposited on quartz substrates by atmospheric pressure chemical vapor deposition (APCVD) using titanium tetraisopropoxide (TTIP) at 250 - 450°C. The effects of deposition temperature on the properties of TiO_2 films were investigated. X-ray diffraction (XRD) shows that films deposited at deposition temperature less than 450°C have anatase TiO_2 phase. Mix phase of anatase and rutile appears at deposition temperature 450°C. It is reported that, crystalline orientation of the TiO_2 film greatly depends on the deposition temperature. All the films have a preferred orientation of (101) plane of anatase with highest orientation factor 0.51 at 350°C. Crystallinity of the film increases with increase in the deposition temperature. Minimum crystallite size of 29.8 nm at 250°C has been estimated using Scherrer's formula. Energy dispersive spectroscopy (EDAX) measurement indicated the presence of Ti and O with no impurities. The results of scanning electron microscopy (SEM) show crack-free, uniform and dense films with slight increase in surface roughness with increasing deposition temperature. TiO_2 films with good transmittance in the range of ~ 56% to ~87% were successfully deposited on quartz substrate by APCVD using TTIP.

(Received December 19, 2007; accepted November 27, 2008)

Keywords: Titanium dioxide (TiO_2), Thin films, Crystalline orientation, Optical transmittance

1. Introduction

Due to the excellent properties, titanium dioxide (TiO_2) thin films have been extensively used in optical thin film device applications. Applications due to its high refractive index [n = 2.5 (anatase) and n = 2.7 (rutile)], and high transparency in the visible and near IR range includes; antireflection coatings, optical waveguides, and recently wide applications in photonic crystal etc. [1-3]. It is a very promising alternative dielectric material for gate dielectric in transistors and dielectric in memory cell capacitor used in DRAMs due to its high dielectric constant (High-k) (ε = 70) [4-6]. A number of deposition techniques have been used to deposit TiO_2 films which include chemical vapor deposition [7-9], sputtering [10], evaporation [11], pulsed laser deposition [12], spray pyrolysis [13], dip coating [14], spin coating [6] etc. Among these techniques, CVD is easy and inexpensive technique for rapid and batch processing of high quality films with better step coverage, large area uniformity, low defect density well controlled stoichiometry etc. Though large work has been reported on CVD [15-17] deposited TiO_2 film very little work has been reported on TiO_2 thin films deposited by APCVD using TTIP.

Qualitative improvement of the TiO_2 films has great importance for the application in the optical devices. Deposition of TiO_2 films with good crystalline orientation is a topic of great interest. Selvaraj et. al. [18] reported sol-gel fabrication of epitaxial and oriented TiO_2 thin films on Si(100), fused silica and rutile(110). Li et. al. [19] reported plasma-sprayed oriented TiO_2 coatings on stainless steel and glass. Watanabe et. al. [20] reported deposition of oriented TiO_2 films on quartz by KrF laser CVD. Crystalline orientation of the TiO_2 film greatly depends on the deposition method and parameters. Very few papers are available on the study of crystalline orientation of TiO_2 films deposited by APCVD using TTIP. In this paper, we report the deposition of TiO_2 films by APCVD using TTIP with preferentially oriented (101) plane of anatase on quartz glass. The effects of deposition temperature on structural phase, crystalline orientation, grain size and optical transmittance of TiO_2 thin films were investigated.

2. Experimental

2.1 Deposition of TiO_2 thin films

The schematic of experimental setup of APCVD system is shown in Fig. 1. In conventional CVD technique, liquid precursor pipeline must be heated to avoid the condensation of precursor vapor inside the pipeline. Instead of using this conventional method, we modified the precursor delivery system by placing the liquid precursor bubbler very close to the reaction chamber. In another modification, we made the provision to inject TTIP vapors near to the quartz boat in order to avoid prior deposition. The system comprises following components - a) quartz tube reactor and boat, b) two zone furnace, c) precursor gases delivery system, d) bubbler contain TTIP in the liquid form, and e) control panel. The reactor is a round quartz tube of 70 cm in length with 4 cm inner diameter. Specially designed quartz boat with 5mm spacing between the adjacent bins is used for holding the substrates inclined in the reactor. The reactor tube is heated and maintained at a constant temperature in the two zone furnace which has the combine zone length of ~10 cm. The hollow stainless steel seals are used to close ends of the quartz tube. A water-cooling arrangement is provided for both seals to protect the O-rings. The

precursors in the gas form and liquid vapor form are introduced in the reactor through ¼" OD stainless steel gas pipelines. Nitrogen (N_2) gas has been used as a carrier gas to carry the TTIP into the reactor. TTIP is stored in stainless steel bubbler which was kept at constant temperature 30°C with the help of paraffin oil bath.

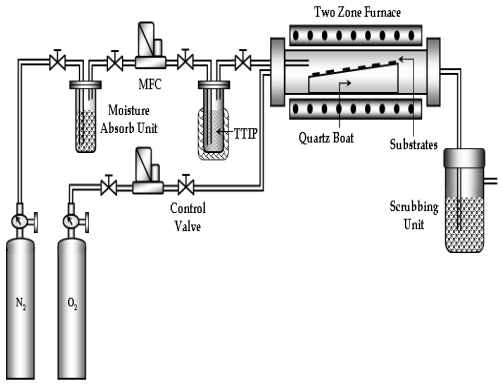

Fig. 1. Schematic of the APCVD system.

We have deposited the TiO_2 films by keeping all processing parameters constant except the deposition temperature. We have carried out various experiments and found that, relatively good quality films obtained at N_2 flow rate 16.66 sccs. TiO_2 films have been deposited on the quartz glass substrates (1cm x 2cm x 1.5mm) by the APCVD system. The substrates were cleaned by ultrasonic bath for 10 minutes followed by dipping in hot trichloroethylene (TCE), acetone, methyl alcohol and deionized water for 10 minutes and then dried in the N_2 gas. The details of the deposition process conditions are listed in Table 1.

Table 1. Process parameters of the TiO_2 films deposited by APCVD using TTIP.

Process parameters	Range
Deposition temperature	250°C – 450°C
N_2 flow rate	16.66 sccs
O_2 flow rate	83.33 sccs
Chamber pressure	1.013×10^5 Pa
Deposition time	10 min
Substrate	Quartz glass

2.2 Characterization techniques

The structural phase and crystallinity of TiO_2 films were determined by X-ray Diffractometer (XRD; Bruker-axs D8) using a Cu Kα radiation source of wavelength λ = 0.1540 nm. Surface morphology was studied using scanning electron microscopy (SEM; JEOL JSM-6360A). SEM based energy dispersive spectroscopy (EDAX) measurements were carried out simultaneously for the determination of the chemical composition of the films. Optical transmission spectra were measured at room temperature using a double beam UV- Vis spectrophotometer (Chemito UV2700) in the wavelength range 200nm to 900nm. Swanepoel's envelope method [21] has been used to determine the thickness from the measured transmission spectra.

3. Results and discussion

Fig. 2 shows X-ray diffraction patterns of the TiO_2 thin films deposited at 250, 300, 350, 400, and 450°C. The film deposited at 250°C has crystalline structure of the anatase phase with corresponding peaks at 2θ values 25.3° [A(101)], 48.1° [A(200)], and 55.1° [A(211)]. These peaks also exist for the film deposited at 300°C but intensities of the peaks for A(101) and A(200) are higher than the film deposited at 250°C. This increase in the peak intensities may be due to the partial conversion of the amorphous to anatase crystallites. Films deposited at 350°C and 400°C also have anatase phase. Film deposited at 450°C shows peaks of anatase phase and a small peak at 2θ value 27.6° [R(110)]. This indicates the anatase-to-rutile crystalline transition begins at 450°C. It has been observed that, generally the anatase peak intensities increases with increase in deposition temperature except for the film deposited at 450°C. This is due to the existence of a rutile phase in the film. The onset temperature of thermally activated structural phase transformation was dependent on experimental parameters such as deposition temperature, substrate material and deposition methods [7]. Structural properties of TiO_2 films were compared with the available literature reporting structural properties of TiO_2 films deposited by various types of CVD methods and are tabulated (Table 2). In view of Table 2, anatase and rutile mix structure begins to appear at quite lower deposition temperature than reported in literature.

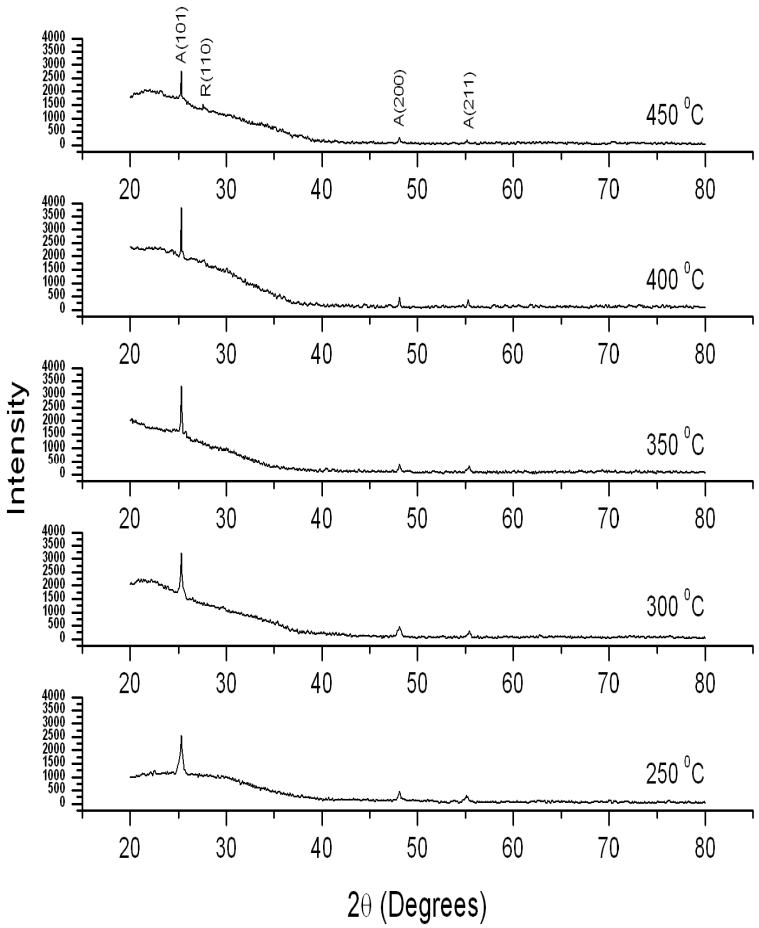

Fig. 2. X-ray diffraction patterns of the TiO_2 thin films deposited by varying deposition temperature.

Table 2. Comparison of structural properties of TiO_2 films deposited by various types of CVD methods.

Author (Ref.)	**Deposition Technique**	**Precursors**	**Substrate**	**Temperature***	**Crystalline Phase**
Present work	APCVD	TTIP + O_2	Quartz	250 – 400°C (Dep.) 450°C (Dep.)	Anatase Anatase + Rutile
O'Neill et. al. [16]	APCVD	$TiCl_4$ + Ethyl Acetate	SiO_2 – coated glass	400 - 500°C (Dep.)	Anatase
Kamata et. al. [22]	CVD	TTIP + O_2	Glass	300°C (Dep.) 400 - 500°C (Dep.)	Amorphous Anatase
Lim et. al. [23]	ALD (Modified CVD)	Tetrakis(dimethylamido) titanium + H_2O	p-type Si or Glass	90 - 210°C (Dep.) 300 - 400°C (Ann.) 500 - 700°C (Ann.) 800°C (Ann.)	Amorphous Anatase Anatase + Rutile Rutile
Maeda et. al. [24]	PECVD	TTIP + O_2	Si or Quartz	350°C (Dep.) 600°C (Ann.) 900°C (Ann.)	Anatase Anatase Rutile
Yang et. al. [25]	PECVD	TTIP + O_2	Si(100)	200 - 350°C (Dep.) 500 - 700°C (Ann.) 800°C (Ann.)	Amorphous Anatase Anatase + Rutile
Won et. al. [7]	MOCVD	TTIP + O_2	Quartz	300°C (Dep.) 600 - 800°C (Ann.) 900°C (Ann.) 1000°C (Ann.)	Anatase Anatase Anatase + Rutile Anatase

* (Dep.) - Deposition / (Ann.) – Annealing Temperature.

Fig. 3 shows FWHM values of the A(101) peak (open squares) and crystallite sizes (full circles) of the TiO_2 films as a function of deposition temperature. Average crystallite size t was determined from the XRD spectra according to the Debye-Scherrer formula [26]

$$t = \frac{0.89\lambda}{\beta \cos\theta}$$

where, λ is the x-ray wavelength (λ = 0.1540 nm), β is the full-width at half-maximum (FWHM) of the diffraction peak and θ is the diffraction angle. Crystalline size increases slightly from 29.8 nm at 250°C to 53.6 nm at 350°C. Above 350°C the nanocrystallites start to grow rapidly due to that they gain more energy than the activation energy for the growth. Decrease in the FWHM and increasing grain size with increasing deposition temperature indicates improved packing density and increasing crystallinity.

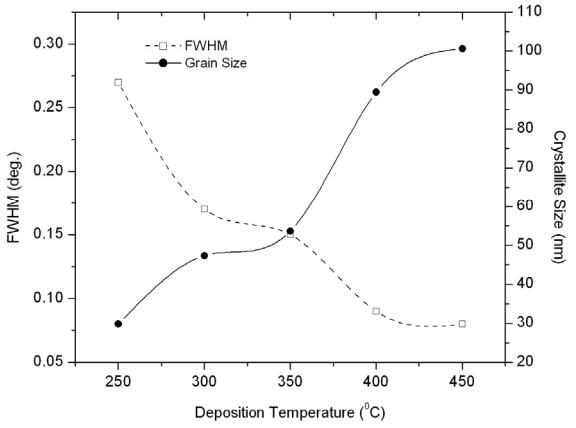

Fig. 3. FWHM values of the A(101) peak (open squares) and calculated crystallite sizes (full circles) of the TiO_2 films as a function of deposition temperature.

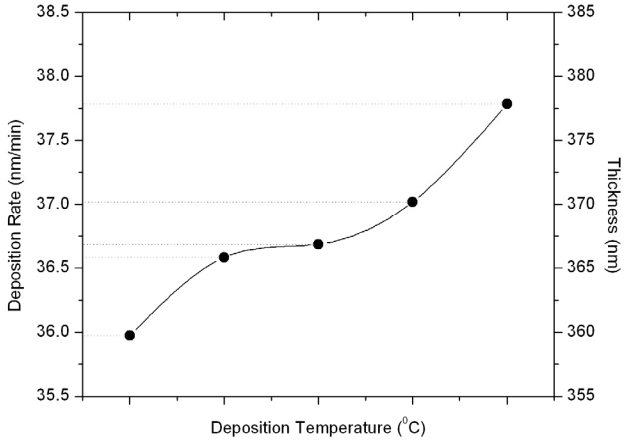

Fig. 4. TiO_2 film deposition rate / thickness as a function of deposition temperature.

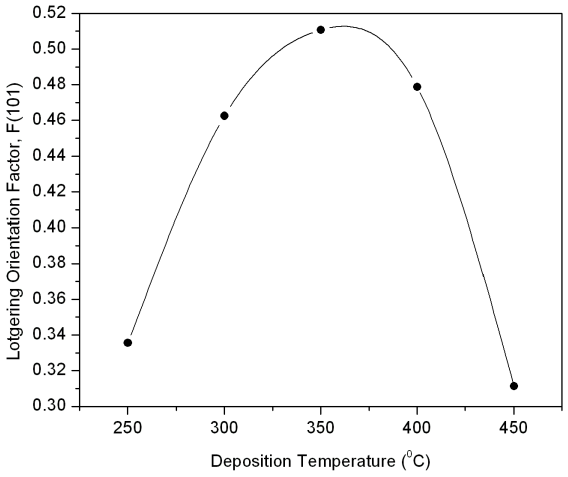

Fig. 5. Lotgering orientation factor, F(101), of TiO_2 films as a function of deposition temperature.

Fig. 4 shows the deposition rate as a function of deposition temperature. Second Y-axis shows thickness of the films. Thickness value of the films ranges from 359nm to 377nm. It has been observed that deposition rate increases with the increase in deposition temperature. Maximum deposition rate 37.7nm/min has been observed at deposition temperature 450°C. Kamata et. al. [22] reports for CVD deposited TiO_2 films, at any substrate temperature, growth rate approaches maximum with increasing TTIP vapor outlet to substrate distance. In the present work, though growth rate increases with deposition temperature, increase is very small due to small TTIP vapor outlet to substrate distance ~10 mm. Due to this TiO_2 films with narrow thickness range were obtained.

Fig. 5 shows the Lotgering orientation factor [27] of TiO_2 films calculated for A(101) as a function of deposition temperature. From the XRD peak intensities, the degree of orientation can be estimated by using Lotgering orientation factor F, defined as

$$F = \frac{(P - P_0)}{(1 - P_0)}$$

Where, P and P_0 is the ratio of the intensity of A(101) to the sum of the all intensities in a scanned range of 2θ for an oriented deposit and standard in the JCPDS diffraction file, respectively. For an increasing degree of orientation P increases from the value P_0 for the non-oriented sample (F = 0) to an ideally oriented sample (F = 1). Therefore, F is the measure of the degree of orientation. The orientation factor F(101) is 0.34 for the film deposited at 250°C indicates good orientation of (101) plane of anatase. F(101) sharply increases up to 0.46 for the film deposited at 300°C. If we combine the results from XRD, this is due to the partial conversion of amorphous to oriented anatase crystallites. Film deposited at 350°C has best preferential orientation of (101) plane of anatase with F(101) having maximum value 0.51. For the film deposited at 400°C, F(101) slightly decreases (F =

0.49). This is due to small increase in the A(200) and A(211) peak intensities. *F*(101) decreases at 0.31 for film deposited at 450°C. This may be due to the appearance of a small peak at 2θ value 27.6 [R(110)] indicating existence of rutile at 450°C. Film orientation was determined during the initial growing steps and greatly influenced by type of substrate, deposition rate and deposition temperature [18-20]. Watanabe et. al. [20] reported that, the (220) plane of anatase was preferentially oriented parallel to substrate surface when the deposition rate was great; while the (112) plane of anatase was oriented in the same way when the deposition rate was small. In the present work, though deposition rate increases with deposition temperature, rate of increase is very small. Sharply increase in preferential orientation of (101) plane of anatase at 300°C and sharply decrease of it at 450°C may be due to partially crystalline conversion initiated due to the increase in the deposition temperature. Hence, at relatively small deposition rate, preferred orientation of (101) plane of anatase depends upon deposition temperature and initially increases, achieve maximum value and then decreases with increase in the deposition temperature.

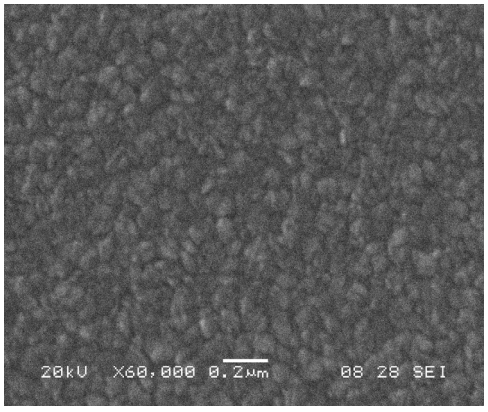

a

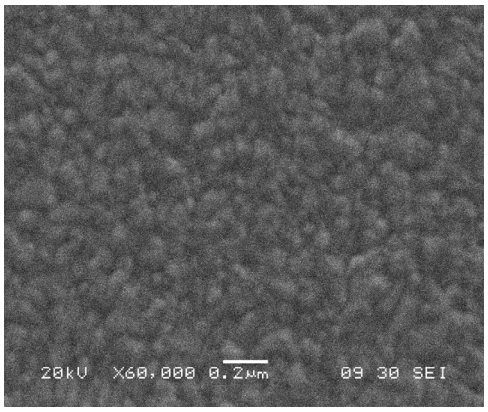

b

Fig. 6. SEM micrographs of the TiO_2 film deposited on quartz substrate at deposition temperature a) 300℃ and b) 350℃.

Fig. 6a and 6b shows the SEM image of the TiO_2 thin film deposited at 300°C and 350°C, respectively. SEM image shows crack-free, uniform and dense films were obtained successfully. As can be seen, crystalline size increases with deposition temperature, which matches with the value evaluated from XRD using Scherrer formula. It is observed that, surface roughness increases with increase in deposition temperature.

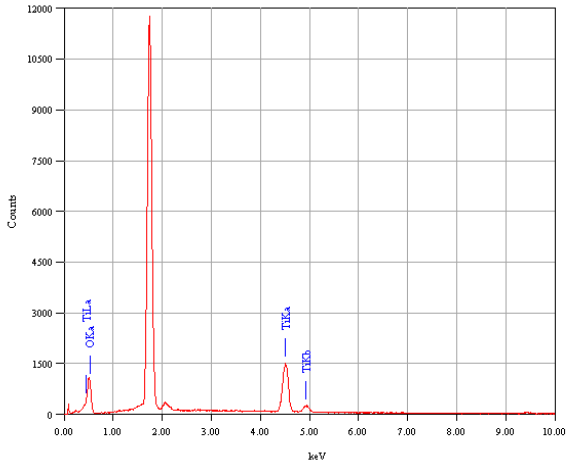

Fig. 7. EDAX spectrum of TiO_2 film deposited at 350℃.

Fig. 7 shows the SEM-EDAX scan for the film deposited at 350°C. X-ray emission line at 1.8 keV arises from quarts substrate, which has large thickness than TiO_2 film. The existence of Ti K_α, Ti K_β, Ti L_α and O K_α X-ray emission lines indicated the presence of titanium and oxygen with no impurities in the film. The Ti:O ratio qualitatively points to the presence of a defect free film surface.

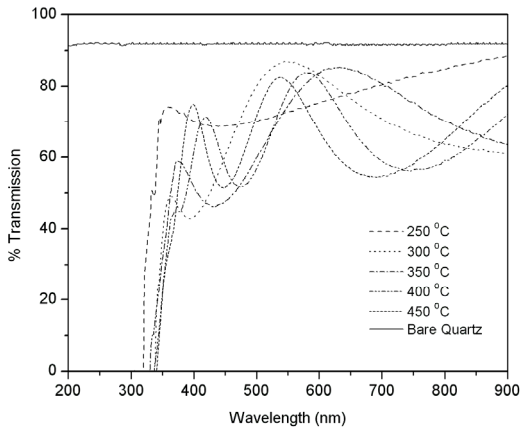

Fig. 8. Optical Transmission spectra as a function of wavelength of TiO_2 thin film deposited on the quartz substrate by varying deposition temperature.

Fig. 8 shows measured optical transmission spectrums of TiO_2 thin films as a function of deposition temperature in the wavelength range 200 nm to 900nm. The transmission of the bare quartz sample is observed

about 92%. All films show good transmittance in the range of ~ 56% to ~87%. The transmittance maxima decrease with increase in the deposition temperature. This is due to increase in surface roughness resulting increasing surface scattering. The absorption edge of the TiO_2 film with lower deposition temperature is observed at a shorter wavelength range than the TiO_2 film with higher deposition temperature. From Fig. 3, crystallite size increases with increase in deposition temperature. Pseudo-"blue shift" of the absorption edge with decrease in deposition temperature may be due to the existence of the smaller crystallites at lower deposition temperature [28]. The transmission spectra of all the films show a sharp decrease in the transmission at approximately 345-375 nm (3.59-3.31 eV), comparable with the reported band gap values for TiO_2 thin film [7,29]. The presence of interference fringes indicates the high refractive index of the films [30].

4. Conclusions

TiO_2 thin films have been successfully deposited on quartz glass by APCVD using TTIP at 250-450°C. Effect of deposition temperature on properties of TiO_2 thin films was examined. XRD shows that only anatase phase exist for the films deposited at less than 450°C. It is found that anatase-to-rutile crystalline transition begins at 450°C. Crystalline orientation of the TiO_2 film greatly depends on the deposition temperature. At relatively small deposition rate preferred orientation of (101) plane of anatase depends upon deposition temperature and initially increases, achieve maximum value and then decreases with increase in the deposition temperature. Best orientation of (101) plane of anatase was obtained at 350°C. Crystallinity of the TiO_2 films increases with increase in the deposition temperature. Minimum crystallite size of 29.8 nm at 250°C has been estimated using Scherrer's formula. EDAX shows the presence of O and Ti with no impurities in the film. Optical transmittance decreases with increase in the deposition temperature due to increase of surface scattering. All the films show good transmittance in the range of 56% to 87%.

References

[1] X. Wang, M. Fujimaki, K. Awazu, Optics Express **13**, 1486 (2005).
[2] K. Narasimha Rao, Opt. Eng. **41**, 2357 (2002).
[3] R. Harbers, P. Strasser, D. Caimi, R. F. Mahrt, N. Moll, D. Erni, W. Bachtold, B. J. Offrein, U. Scherf, J. Opt. A: Pure Appl. Opt. **8**, S273 (2006).
[4] H. –K. Ha, M. Yoshimoto, H. Koinuma, B. –K. Moon, H. Ishiwara, Appl. Phys. Lett. **68**, 2965 (1996).
[5] K. –T. Lin, J. –M. Wu, Jpn J. Appl. Phys. **43**, 232 (2004).
[6] N. B. Chaure, A. K. Ray, R. Capan, Semicond. Sci. Technol. **20**, 788 (2005).
[7] D. –J. Won, C. –H. Wang, H. –K. Jang, D. –J. Choi, Appl. Phys. A **73**, 595 (2001).
[8] G. A. Battiston, R. Gerbasi, A. Gregori, M. Porchia, S. Cattarin, G. A. Rizzi, Thin Solid Films **371**, 126 (2000).
[9] S. S. Huang, J. S. Chen, J. Mater. Sci. **13**, 77 (2002).
[10] M. Stamate, I. Vascan, I Lasar, G. Lasar, I. Caraman, M. Caraman, J. Opt. Adv. Mater. **7**, 771 (2005).
[11] K. Narasimha Rao, S. Mohan, J. Vac. Sci. Technol. A **8**, 3260 (1990).
[12] X. –S. Zhou, Y. –H. Lin, B. Li, L. –J. Li, J. –P. Zhou, C. –W. Nan, J. Phys. D **39**, 558 (2006) .
[13] A. Conde-Gallardo, M. Guerrero, N. Castillo, A. B. Soto, R. Fragoso, J. G. Cabanas-Moreno, Thin Solid Films **473**, 68 (2005).
[14] H. Yang, X. Zhang, Q. Tao, A. Tang, J. Optoelectron. Adv. Mater. **9**, 2493 (2007).
[15] A. Mills, S. –K. Lee, A, Lepre, I. P. Parkin, S. A. O'Neill, J. Photochem. Photobilo. Sci. **1**, 865 (2002).
[16] S. A. O'Neill, R. J. H. Clark, I. P. Parkin, N. Elliott, A. Mills, Chem. Mater. **15**, 46 (2003) .
[17] S. A. O'Neill, I. P. Parkin, R. J. H. Clark, A. Mills, N. Elliott, J. Mater. Chem. **13**, 56 (2003) .
[18] U. Selvaraj, A. V. Prasadarao, S. Komarneni, R. Roy, J. Am. Ceram. Soc. **75**, 1167 (1992).
[19] J. F. Li, C. X. Ding, J. Mater. Sci. Lett. **17**, 1747 (1998).
[20] A. Watanabe, Y. Imai, Thin Solid Films **348**, 63 (1999).
[21] R. Swanepoel, J. Phys. E: Sci. Instrum. **16**, 1214 (1983).
[22] K. Kamata, K. Maruyama, S. Amano, H. Fukazawa, J. Mater. Sci. Lett. **9**, 316 (1990).
[23] G. T. Lim, D. –H. Kim, Thin Solid Films **498**, 254 (2006).
[24] M. Maeda, T. Watanabe, Thin Solid Films **489**, 320 (2005).
[25] W. Yang, J. Marino, A. Monson, C. A. Wolden, Semicond. Sci. Technol. **21**, 1573 (2006).
[26] B. D. Cullity, S. R. Stock, Elements of X-ray diffraction, Printice Hall, Englewood Cliffs, NJ, (2001).
[27] F. K. Lotgering, J. Inorg. Nucl. Chem. **9**, 113 (1959).
[28] J. Yu, X. Zhao, Q. Zhao, J. Mater. Sci. Lett. **19**, 1015 (2000).
[29] Y. Gao, Y. Masuda, Z. Peng, T. Yonezawa, K. Koumoto, J. Mater. Chem. **13**, 608 (2003).
[30] K. Bange, C. R. Ottermann, O. Anderson, U. Jeschkowski, M. Laube, R. Feile, Thin Solid Films **197**, 279 (1991).

*Corresponding author:drpatil@yahoo.com